2016

Assessment Of DR-55 As A Drop-In Replacement For R410A

Bo Shen
Oak Ridge National Laboratories, United States of America, shenb@ornl.gov

Omar Abdelaziz
Oak Ridge National Laboratories, United States of America, abdelazizoa@ornl.gov

Lane Liudahl
Oak Ridge National Laboratories, United States of America, lliudahl@trane.com

Assessment of DR-55 as a Drop-In Replacement for R-410A

Bo Shen[1]*, Omar Abdelaziz[1], Lane Liudahl[2]

[1]Building Technologies Research and Integration Center, Oak Ridge National Laboratory
One Bethel Valley Road, P.O. Box 2008, MS-6070, Oak Ridge, TN 37831-6070
[2] Ingersoll Rand.

Email: shenb@ornl.gov, Telephone: 1-8655745745

ABSTRACT

R410A has no ozone depletion potential (ODP), and is the most commonly used refrigerant in vapor compression systems for space cooling and heating applications. However, it has significant global warming potential with GWP higher than 1900. To mitigate the global warming effect, industry and research institutes are actively pursuing a replacement for R-410A with the following attributes, much lower GWP along with similar or higher efficiency and capacity. DR-55 (aka R452B) is a design-compatible refrigerant replacement for R-410A. It decreases the GWP by 70%, and has lower working pressure, comparable discharge temperature, and uses the same lubricant, tubing, and valves. In this study, we experimentally evaluated the performance of DR-55 as a drop-in replacement for R-410A in a high efficiency rooftop air conditioning unit. The experimental results demonstrated that DR-55 led to 5% higher efficiency at the working conditions of Integrated Energy Efficiency Rating (IEER). DR-55 also showed significantly better high ambient performance from 95°F to 125°F. In addition to the experimental study, we used the DOE/ORNL Heat Pump Design Model to model a rooftop unit (RTU) using R-410A and DR-55, respectively. The model results were compared to the laboratory measurements. The model validation demonstrates that the refrigerant heat transfer and pressure drop correlations, developed for conventional refrigerants like R-410A, are usable for DR-55. Also, a converted compressor model for DR-55, i.e. reducing volumetric and isentropic efficiencies as a function of the suction and discharge pressures from an R-410A compressor map can predict the compressor mass flow rate and power accurately.

1. INTRODUCTION

The US Department of Energy released a new high-efficiency design specification for commercial air conditioners with 10-ton (35.2 kW) to 20-ton (70.4 kW) capacity. It targets a high-performance Integrated Energy Efficiency Rating (IEER) of 18.0 (Btu/h/W) (Reference: High Performance Rooftop Unit Challenge). ANSI/AHRI 340/360 is the standard for rating IEER. It puts significant weighting on part-load performances as shown in Equation 1, i.e. A - 2% weight from EER at 100% capacity and 95°F (35°C) ambient temperature, B - 61.7% weight for EER at 75% capacity and 81.5°F (27.5°C), C - 23.8% weight for EER at 50% capacity and 68°F (20.0°C), D – 12.5% weight for EER at 25% capacity and 65°F (18.3°C). This requires smooth capacity modulation with varying air and refrigerant flow rates, and full utilization of all the heat exchanger surface areas at part-load conditions. Advanced components need to be used to meet the design targets, like micro-channel heat exchangers, high efficiency fans and compressors, etc.

$$\mathbf{IEER = 0.020*A + 0.617*B + 0.238*C + 0.125*D} \quad (1)$$

More than half of U.S. commercial building space is cooled by Rooftop Air Conditioners (RTU). Existing rooftop HVAC units consume more than 1.3% of the total US energy annually (1.0 Quad source energy, EIA 2015). If built to meet the target specification > 18 IEER, these units would reduce energy use by as much as 50% over current standards. Nationwide, if all 10 to 20-ton RTUs met the IEER goal, businesses would save over $1 billion each year in energy costs.

The use of hydrofluorocarbon (HFC) refrigerants as non-ozone-depleting alternatives for air-conditioning and refrigeration equipment was adopted by the developed countries during the ozone-depleting substances (ODS) phase-out as described in the Montreal Protocol. Unfortunately, most of the HFCs employed have higher global warming potential (GWP) compared to the refrigerants they replaced. For example, R-410A has a GWP (AR5) of 1924, which is thousands of times higher than natural substances like CO2. HFCs currently account for only 1% of greenhouse gas emissions, but their use is growing rapidly, by as much as 10 to 15% per year, primarily because of

their use as replacements for ODS and the increasing use of air conditioners globally, as reported by Ramanathan and Xu (2010 and 2013). As such, finding suitable lower GWP replacements for HFC and hydrochlorofluorocarbon (HCFC) refrigerants is timely. Furthermore, the low GWP refrigerant candidates are expected to facilitate a higher or similar efficiency level than the present HFC refrigerants, in order to reduce indirect global warming effects caused by electricity generation.

DR-55 recently emerged as a promising candidate to replace R-410A. It decreases the GWP by 70%, and slightly increases the efficiency when used in existing R410A-based equipment. Table 1 compares some key parameters of R-410A, R-32 and DR-55. In the table, the temperature glides in the condenser were calculated as the difference between the saturated vapor temperature and the saturated liquid temperature at the pressure corresponding to 115°F (46.1°C) dew point; and glides in the evaporator was calculated at the pressure corresponding to 50°F (18°C) dew point.

Table 1. Alterative Low GWP Replacements for R-410A

Refrigerant	GWP AR4[c]	GWP AR5 [d]	Safety Class	Glide in Condenser [K]	Glide in Evaporator [K]	Critical Temperature [C]
R-410A[a]	2088	1924	A1	0.1	0.1	71.34
R-32	675	677	A2L	0.0	0.0	78.12
DR-55[b]	698	676	A2L	1.2	1.3	79.68

[a.] R-410A has mass-based compositions of R-32 (0.5)/R-125 (0.5).
[b.] DR-55 has mass-based compositions of R-32 (0.67)/R-125 (0.07)/R-1234yf (0.26).
[c.] AR4 can be referred to Solomon et al., 2007.
[d.] AR5 can be referred to Myhre et al., 2013.

DR-55 has a similar GWP as R-32, but is less flammable. DR-55 contains, on mass-basis, 26% of R-1234yf, which is known to be less flammable than R-32, and also, it has 7% of R-125, which is actually the fire suppression agent in this mixture. DR-55 provides a good balance between the GWP and flammability for commercial unitary air conditioning systems, which tend to have relatively large inner volume and charge mass.

2. Thermodynamic Properties

The temperature-enthalpy diagram of a refrigerant illustrates two critical properties: its span between the saturated liquid line and saturated vapor line (i.e. latent heat of vaporization) and critical temperature (working range). Volumetric vaporization heat, i.e. latent heat × vapor density at an average saturation temperature of dew point and bubble point, indicates the evaporating capacity per volumetric flow rate. Refrigerants with smaller volumetric vaporization heat have reduced cooling capacities at the same average saturation temperature and compressor displacement volume.

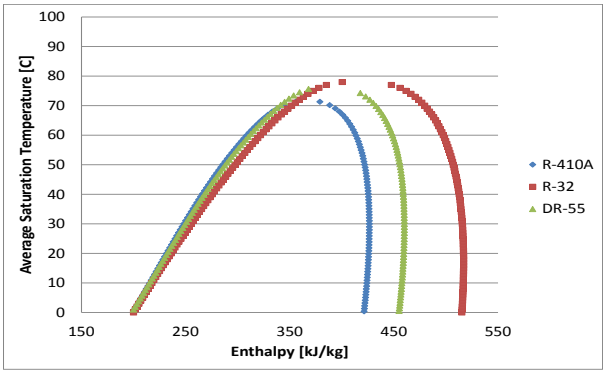

Figure 1: Temperature-Enthalpy plot

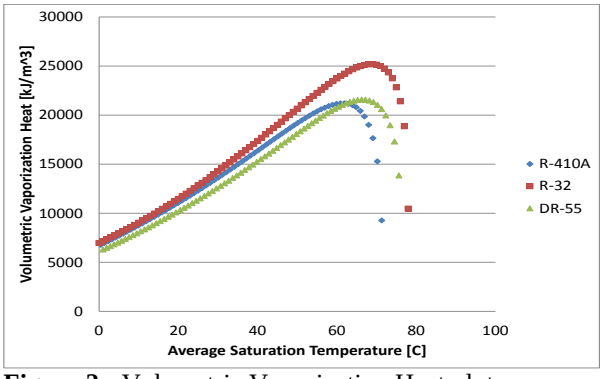

Figure 2: Volumetric Vaporization Heat plot

Figure 1 illustrates the temperature-enthalpy diagram of R-410A, DR-55 and R-32. DR-55 and R-32 have wider domes and higher critical temperatures than R-410A, indicating that they are better refrigerants for high ambient operation. Figure 2 illustrates the volumetric vaporization heats vs. the average saturation temperature. It shows that DR-55 has the smallest volumetric vaporization heat, and thus R-410A and R-32 will likely lead to larger cooling capacities than DR-55 at the same evaporating temperature and compressor displacement.

Figure 3 shows the saturation temperature vs. density of the three refrigerants. It shows that DR-55 and R-32 have lower saturated vapor densities at the same suction saturation temperature. It indicates that they have reduced compressor mass flow rate and power consumption at a given volumetric compressor displacement. Figure 4 plots pressure as a function of the saturated vapor and liquid temperatures. It can be seen that DR-55 has a consistent, negligible temperature glide around 1.2 K (2 R) over the whole range. DR-55 is inclined to work at a lower pressure compared to R-410A at the same saturated vapor temperature. R-32 has a similar saturation pressure-temperature curve as R-410A.

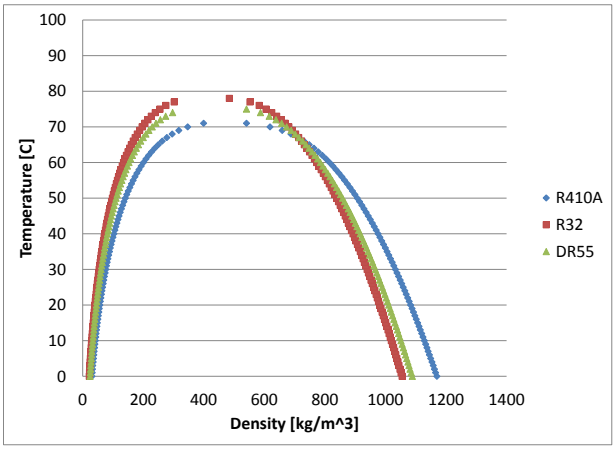

Figure 3: Saturation temperature-density curves

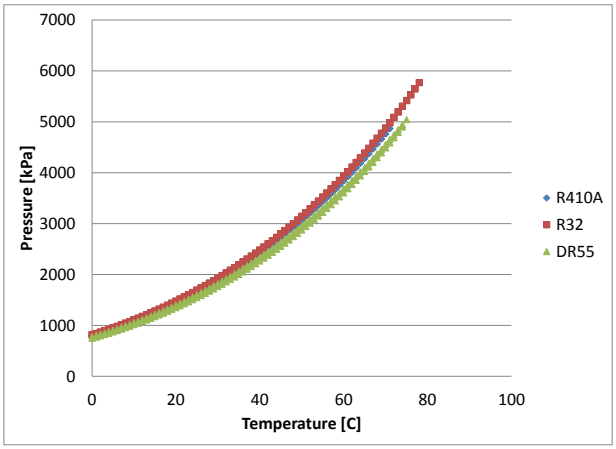

Figure 4: Saturation pressure-temperature curves

3. EXPERIMENTAL STUDY

We conducted a soft-optimized investigation, using DR-55 to replace R-410A in a high efficiency RTU, developed in collaboration with the Trane Company. The RTU uses a variable-speed compressor, a thermo-expansion valve (TXV) to control the evaporator exit superheat degree at 10 R (5.6 K), variable-speed indoor blower and condenser fans. It has a fin-&-tube evaporator and a micro-channel condenser. The indoor air flow rate was varied to maintain a constant supply air temperature at 60°F (15.6°C). The condenser air flow was controlled as a function of the compressor speed. Two adjustments were made in the RTU when using DR-55. The first was to decide the system charge for getting the same condenser subcooling degree as R-410A, i.e. 17 R (9.4 K) at 95°F (35°C), with running the compressor at its full capacity. As a result, DR-55 required 10% less charge than R-410A. The second was to turn down the TXV's fixed opening slightly. With these settings, DR-55 reached approximately the same rated cooling capacity as R-410A with the variable-speed compressor at its highest speed.

Steady state performance tests of the RTU were conducted for the two refrigerants, at the four IEER rating conditions. The compressor was modulated to match the required capacities of Conditions A, B and C. At condition D, the compressor couldn't turn down to the required 25% capacity, and thus, cyclic loss was calculated, per ANSI/AHRI 340/360. Cooling capacities were measured at the air side by installing a grid of thermocouples and relative humidity sensors at the return and supply sides of the indoor air flow path, and individual component power consumptions were monitored using watt transducers. Furthermore, the refrigerant pressure and temperatures were measured using pressure transducers and inserted temperature probes. An RTU using R-410A is known to have noticeable performance degradation at high ambient temperatures, when its discharge pressure approaches the critical point. To investigate these issues, high ambient tests were conducted, by running the compressor at its full capacity and increasing the ambient temperature from 95°F to 125°F (35°C to 51.7°C).

Figure 5 shows ratios of EERs of DR-55 versus R410A at the four IEER ambient conditions and capacity levels. These results indicate that, with DR-55, the RTU's IEER increases by 5%. Figure 6 illustrates compressor discharge temperature vs. ambient temperature for both R410A and DR-55. One can see that, at ambient temperatures from 95°F (35°C) to 125°F (51.7°C), DR-55 led to around 13R (7.2K) higher discharge temperatures than with the original R410A. At the 125°F (51.7°C) ambient condition, the discharge temperature of DR-55 was 233°F (111.7°C), still far below the high temperature limit suggested by the compressor manufacturer.

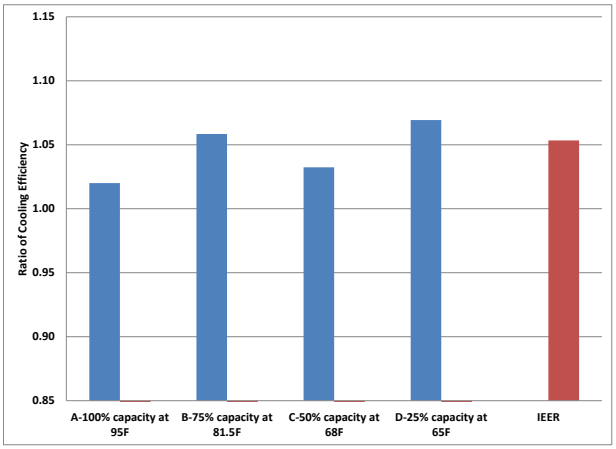

Figure 5: Ratios of EERs and IEER, at four IEER rating conditions, DR-55 vs. R-410A

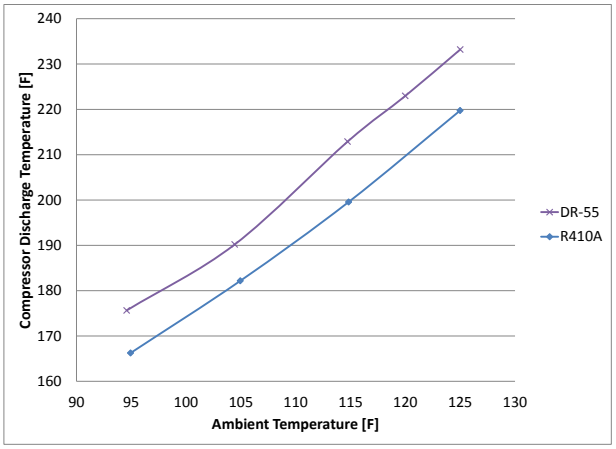

Figure 6: Compressor discharge temperature at high ambient temperatures

Figures 7 and 8 illustrate cooling capacity and efficiency degradation ratios, as a function of ambient temperature from 95°F to 125°F (35°C to 51.7°C). The degradation ratios were obtained as measured air-side cooling capacities and EERs (Energy Efficiency Ratio), divided by the rated value at 95°F (35°C) for each refrigerant. It can be seen that the capacity and EER of R-410A degrade faster than DR-55, as it approaches its critical point.

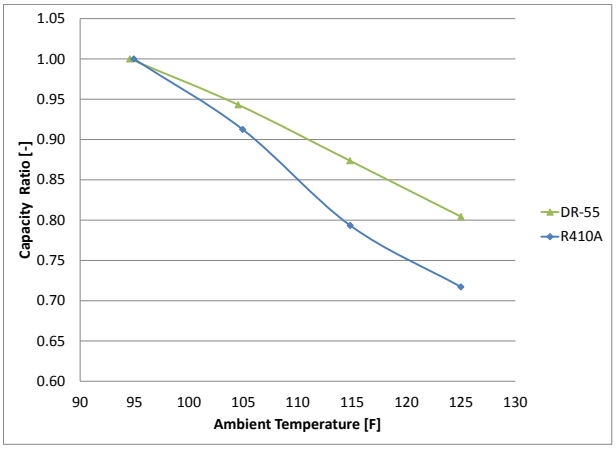

Figure 7: Capacity degradation with ambient

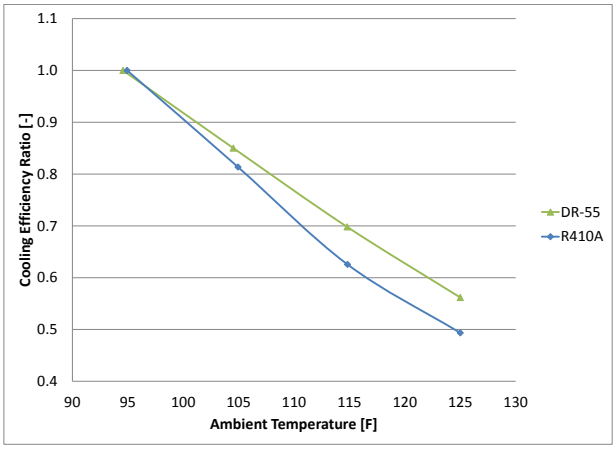

Figure 8: Efficiency degradation with ambient

4. MODEL DESCRIPTION

The DOE/ORNL Heat Pump Design Model (HPDM, Rice 1997 and Shen 2014) was used to model the RTU with R-410A and DR-55. HPDM is a well-recognized, public-domain HVAC equipment modelling and design tool. It has a free web interface to support public use, which has been accessed over 300,000 times by US and worldwide engineers. Some features of the HPDM, related to this study, are introduced below:

Compressor model:

AHRI 10-coefficient compressor maps (ANSI/AHRI 540-99, 2010) are used to calculate mass flow rate and power consumption, and enable calculation of the refrigerant-side vs. air-side energy balance from inlet to outlet by inputting a compressor shell loss ratio relative to the power input. We also consider the actual suction state to correct the map mass flow prediction using the method of Dabiri and Rice (1981). For modeling a variable-speed compressor, HPDM accepts multiple sets of mass flow and power curves at various speed levels, and does linear interpolation between speed levels.

For this study, we obtained the original compressor map, developed for R-410A. For modeling alternative refrigerants, it is assumed that the compressor would maintain the same volumetric and isentropic efficiencies at the same suction and discharge pressures. Thus, the efficiencies were reduced from the original R-410A map as a function of the suction and discharge pressures. The volumetric efficiency is defined in Equation 2, and isentropic efficiency is shown in Equation 3.

$$m_r = Volume_{displacement} \times Speed_{rotation} \times Density_{suction} \times \eta_{vol} \quad (2)$$

$$Power = m_r \times (H_{discharge,s} - H_{suction})/\eta_{isentropic} \quad (3)$$

Where m_r is compressor mass flow rate; $Power$ is compressor power; η_{vol} is compressor volumetric efficiency; $\eta_{isentropic}$ is compressor isentropic efficiency; $H_{suction}$ is compressor suction enthalpy; $H_{discharge,s}$ is the enthalpy obtained at the compressor discharge pressure and suction entropy.

Heat Exchanger models:

Segment-to-segment fin-&-tube heat exchangers: HPDM uses a segment-to-segment modeling approach, which divides a single tube into numerous mini segments. Each tube segment has individual air side and refrigerant side entering states, and considers possible phase transition; ε-NTU approach is used for heat transfer calculations within each segment. Air-side fin is simplified as an equivalent annular fin. Both refrigerant and air-side heat transfer and pressure drop are considered; the coil model can simulate arbitrary tube and fin geometries and circuitries, any refrigerant side entering and exit states, misdistribution, and accept two-dimensional local air side temperature, humidity and velocity inputs; the tube circuitry and 2-D boundary conditions are provided by an input file. For modeling a condenser, the flow-pattern-dependent heat transfer correlation published by Thome (2003a,b) is used to calculate the condenser two-phase heat transfer coefficient. The pressure drop correlation published by Kedzierski (1999) is used to model the two-phase pressure drop. In addition to the functionalities of the segment-to-segment fin-tube condenser, the evaporator model is capable of simulating dehumidification process. The method of Braun, et al. (1989) is used to simulate cases of water condensing on an evaporating coil, where the driving potential for heat and mass transfer is the difference between enthalpies of the inlet air and saturated air at the refrigerant temperature. The heat transfer correlation published by Thome (2002) is used to calculate the evaporator two-phase heat transfer coefficient. Air side heat transfer correlations were obtained from Wang (2001), specific to different fin types, e.g. louvered fin, wavy fin, slit fin, etc. The segment-to-segment modeling approach is a natural fit to handle refrigerant mixtures having a temperature glide, since each mini-segment has a constant saturation temperature, and the heat exchanger model captures the glide by accounting for temperature change segment-to-segment in the flow path. The air side and refrigerant side heat transfer calculations can be adjusted using multipliers to match measured data.

Segment-to-segment micro-channel condenser: The model uses a segment-to-segment modeling approach; each micro-channel port segment has individual air-side and refrigerant-side entering states, and considers possible phase transition; the coil model can simulate arbitrary port shapes (round, triangle, etc.), fin geometries and circuitries (serpentine, slab, etc.). The heat transfer correlation published by Dobson (1998) is used to calculate the condenser two-phase heat transfer coefficient. The Kedzierski (2000) correlation is used to calculate the two-phase pressure drop. Air side fins are assumed as straight fins, using the heat transfer correlation published by Kim and Bullard (2002).

Expansion Devices:

The compressor suction superheat degree and condenser subcooling degree are explicitly specified. As such, the expansion device is not solved here – a simple assumption of constant enthalpy process is taken.

Fans and Blowers:

Single-speed fan: the air flow rate and power consumption were direct inputs from the laboratory measurements.

Refrigerant Lines:

Heat transfer in a refrigerant line is ignored and the pressure drop is calculated using a turbulent flow model, as a function of the refrigerant mass flux.

Refrigerant Properties:

Interface to REFPROP 9.1 (Lemmon et al., 2010): We programmed interface functions to call REFPROP 9.1 directly; our models accept all the refrigerant types in the REFPROP 9.1 database, and also we can simulate a new refrigerant by making the refrigerant definition file according to the REFPROP 9.1 format. To speed up the property calculation, we have an option to generate property look-up tables, using REFPROP 9.1; our program uses 1-D and 2-D cubic spline interpolation algorithms to calculate refrigerant properties via reading the look-up tables, this would greatly boost the calculation speed, given the same accuracy.

5. MODEL VALIDATION

At the current stage, the thermodynamic and transport properties of DR-55 are available. However, fundamental studies for evaluating its heat transfer and pressure drop behaviors and refrigerant-specific compressor maps are still absent. Thus this simulation study intends to validate two points. One point is to verify whether the heat transfer and pressure drop correlations of HPDM, mainly developed for conventional refrigerants, e.g. R-410A, R-22, etc., are suitable to predict the DR-55 performance. As mentioned, the compressor model converted the R-410A compressor map to volumetric and isentropic efficiencies of DR-55 vs. the suction and discharge pressures. Therefore, the other point is to evaluate whether the compressor model is adequate to predict the compressor power consumption and cooling capacities of DR-55 under various operation conditions.

For the simulation study, we first calibrated the system model of R-410A to match the measured suction and discharge saturation temperatures at 95°F (35°C), i.e. IEER condition A, by adjusting the air side heat transfer correction multipliers in the evaporator and condenser models, while keeping the refrigerant side heat transfer calculations unchanged. Using the single set of calibration factors, the model was used to predict performances at other test points of R-410A, as well as DR-55. At each simulation point, the measured condenser subcooling degree, evaporator exit superheat degree, indoor and outdoor air flow rates were used as inputs to the model. The compressor shell loss was assumed as 10% relative to the compressor power.

Figures 9 and 10 show deviations between the predicted and measured values, of suction and discharge saturated vapor temperature. It can be seen, that the same set of correlations and heat transfer calibration factors led to the same level of prediction accuracy for R-410A and DR-55. It indicates that the heat transfer and pressure drop correlations of R-410A can also be used for DR-55.

Figure 11 compares predicted cooling capacities to the measured air side capacities at ambient temperatures from 65°F (18.3°C) to 81.5°F (27.5°C). The capacity prediction deviations are all within ±6%, implying that the R-410A compressor map and converted DR-55 compressor model are able to calculate the refrigerant mass flow rates accurately. It should be mentioned that we didn't compare the capacities at the ambient temperatures higher than 95°F (35°C), because the RTU's cabinet heat losses were significant (>10% air side cooling capacity lost to the ambient) at high ambient temperatures. Figure 12 compares predicted compressor powers to the measured values at ambient temperatures from 65°F (18.3°C) to 125°F (51.7°C). It can be seen that the converted compressor model predicted the DR-55 power consumptions more accurately than the compressor map predicted the R-410A performance. This demonstrates that the DR-55 compressor model, converted from the R-410A compressor map,

can be adopted to predict the compressor mass flow rate and power consumption, before a DR-55 specific map is developed.

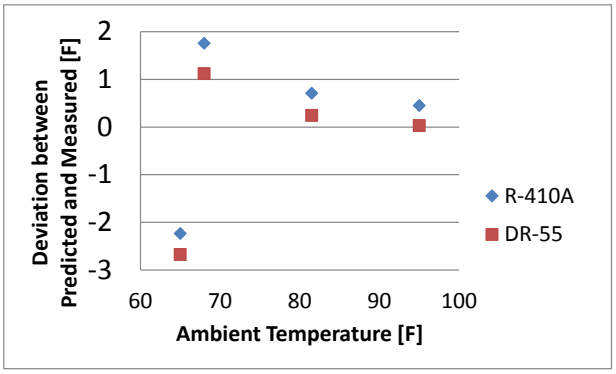

Figure 9: Deviation between predicted and measured suction saturation temperatures vs. ambient temperature

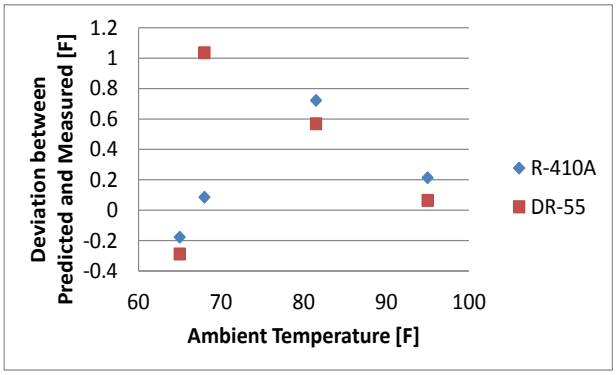

Figure 10: Deviation between predicted and measured discharge saturation temperatures vs. ambient

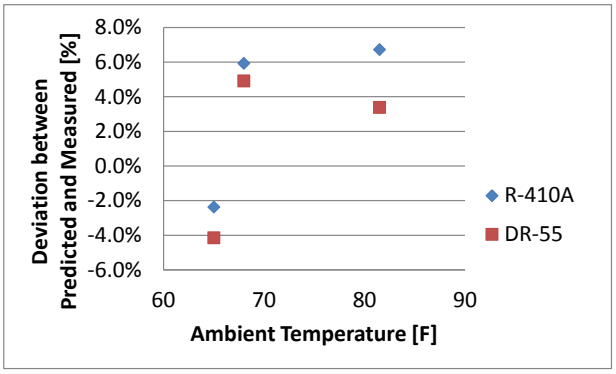

Figure 11: Deviation between predicted and measured air side capacities vs. ambient temperature

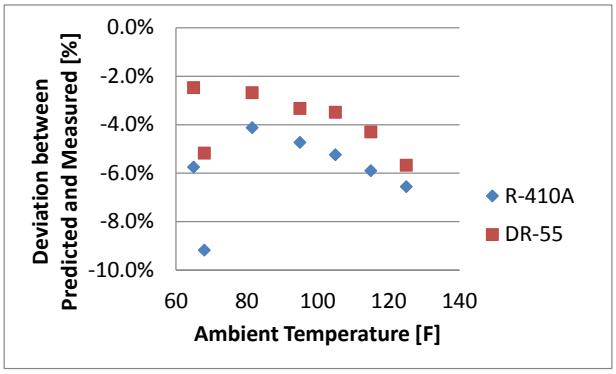

Figure 12: Deviation between predicted and measured compressor powers vs. ambient temperature

6. SUMMARY

In general, DR-55 is a better refrigerant than R-410A from all the perspectives. It is a very promising, low GWP candidate to replace R-410A for commercial unitary systems. The advantages of DR-55 can be summarized as below:

1. Much lower GWP than R-410A: 675 vs. 1924.
2. Better system efficiency and similar capacity in the case of a drop-in replacement: ~5% higher IEER in the equipment tested in this study.
3. 10% less charge is required than R410A.
4. Direct design-compatible replacement for R410A: Lower pressure refrigerant compared with R-32, comparable discharge temperature, same lubricant, tubing, valves, and seals. It only needs minor adjustments of the expansion devices.
5. Significantly better high-ambient performance in the equipment tested in this study: less capacity and efficiency degradations at high ambient temperatures, while having a tolerable increase in compressor discharge temperature.

From the model validation, one can see that the refrigerant heat transfer and pressure drop correlations, developed for conventional refrigerants like R-410A, are usable for DR-55 with good accuracy. In addition, the converted compressor model for DR-55, i.e. reducing volumetric and isentropic efficiencies as a function of the suction and discharge pressures from an R-410A compressor map can predict the compressor mass flow rate and power fairly well.

By looking at the thermodynamic properties, R-32 appears the best low GWP refrigerant candidate. However, because it is more flammable than DR-55, R-32 is less likely to be the final selection to replace R-410A in large commercial packaged units. In addition, R-32 has a wider dome which would lead to higher compressor discharge temperature.

REFERENCES

ANSI/AHRI Standard 540-99, 2010, "Positive Displacement Refrigerant Compressors and Compressor Units", Air-Conditioning and Refrigeration Institute, Arlington, VA

ANSI/AHRI Standard 340/360, 2010, "Performance Rating of Commercial and Industrial Unitary Air-Conditioning and Heat Pump Equipment", Air-Conditioning, Heating, and Refrigeration Institute, Arlington, VA

Braun. J.E., Klein. S.A, and Mitchell, J.W., 1989, "Effectiveness models for cooling towers and cooling coils", ASHRAE Transactions, 95(2), pp. 164-174.

EIA (US Energy Information Administration), 2015. 2012 Commercial Buildings Energy Consumption Survey (CBECS), Tables B1 and B2. http://www.eia.gov/consumption/commercial/data/2012/#summary (accessed September 2015).

Dabiri, A. E. and C.K. Rice, 1981. "A Compressor Simulation Model with Corrections for the Level of Suction Gas Superheat," ASHRAE Transactions, Vol. 87, Part 2, pp.771-782.

Dobson M. K. and Chato J. C., 1998 "Condensation in Smooth Horizontal Tubes", Journal. Heat Transfer 120(1), 193-213 (Feb 01, 1998)

Myhre G., D. Shindell, F.-M. Bréon, W. Collins, J. Fuglestvedt, J. Huang, D. Koch, J.-F. Lamarque, D. Lee, B. Mendoza, T. Nakajima, A. Robock, G. Stephens, T. Takemura, and H. Zhang (2013). "Anthropogenic and Natural Radiative Forcing," in Climate Change 2013: The Physical Science Basis. Contribution of Working Group I to the Fifth Assessment Report of the Intergovernmental Panel on Climate Change. T. F. Stocker, D. Qin, G.-K. Plattner, M. Tignor, S. K. Allen, J. Boschung, A. Nauels, Y. Xia, V. Bex and P. M. Midgley, eds. Cambridge University Press, Cambridge, United Kingdom, and New York, NY, USA. Available at https://www.ipcc.ch/pdf/assessment-report/ar5/wg1/WG1AR5_Chapter08_FINAL.pdf. Accessed October 2015.

Kedzierski, M. A., and Choi J. Y., "A generalized pressure drop correlations for evaporation and condensation of alternative refrigerants in smooth and micro-fin tubes" NISTIR 6333, 1999

Kim Man-Hoe, Bullard Clark W., 2002, "Air-side thermal hydraulic performance of multi-louvered fin aluminum heat exchangers.", International Journal of Refrigerant, No. 25, pp 390-400.

Lemmon Eric W., Huber Marcia L. (2010) "NIST Reference Fluid Thermodynamic and Transport Properties Database (REFPROP): Version 9.1", http://www.nist.gov/srd/upload/REFPROP9.PDF

Rice, C. K., 1997. "DOE/ORNL Heat Pump Design Model, Overview and Application to R-22 Alternatives",3rd International Conference on Heat Pumps in Cold Climates, Wolfville, Nova Scotia, Canada, Aug. 11-12, 1997; Caneta Research, Inc., Mississauga, Ontario, Canada, November, pp.43-66.

Ramanathan and Y. Xu (2010). "The Copenhagen Accord for Limiting Global Warming: Criteria, Constraints, and Available Avenues," Proc. Natl. Acad. Sci. USA 107, 8055–8062.

Shen, B. and Rice, C. K., 2014, HVAC System Optimization with a Component Based System Model – New Version of ORNL Heat Pump Design Model, Purdue HVAC/R Optimization short course, International Compressor & refrigeration conferences at Purdue, Lafayette, USA, 2014; web link: http://hpdmflex.ornl.gov/hpdm/wizard/welcome.php

Solomon, S. D. Qin, M. Manning, Z. Chen, M. Marquis, K. B. Averyt, M. Tignor, and H. L. Miller, eds., 2007, Climate Change 2007: The Physical Science Basis. Contribution of Working Group I to the Fourth Assessment Report of the Intergovernmental Panel on Climate Change (2007). Cambridge University Press, Cambridge, United Kingdom, and New York, NY, USA; Section 2.10.2: Direct Global Warming Potentials. 2013.Available at https://www.ipcc.ch/publications_and_data/ar4/wg1/en/contents.html. Accessed October 2015.

Thome J.R. and Jean Ei Hajal, 2002, "On recent advances in modelling of two-phase flow and heat transfer", 1st Int. Con. on Heat Transfer, Fluid mechanics, and Thermodynamics, Kruger Park, south Africa TJ1, 8-10 April.

Thome J. R., J. El Hajal, and A. Cavallini, 2003a, "Condensation in horizontal tubes, part 1: two-phase flow pattern map", International Journal of Heat and Mass Transfer, 46(18), Pages 3349-3363.

Thome J. R., J. El Hajal and A. Cavallini, 2003b, “Condensation in horizontal tubes, part 2: new heat transfer model based on flow regimes”, International Journal of Heat and Mass Transfer, 46(18), Pages 3365-3387.

Wang, C. C., 2001, "A Comparative Study of Compact Enhanced Fin-and-Tube Heat Exchangers", Int. J. Heat and Mass Transfer, Vol. 44, pp. 3565-3573.

ACKNOWLEDGEMENT

The authors thank Mr. Antonio Bouza, Technology Development Manager for HVAC, WH, and Appliances, Emerging Technologies Program, Buildings Technology Office at the U.S. Department of Energy for supporting this research project.